Supplementary information for: Similarities and Differences between Na^+ and K^+ Distributions around DNA Obtained with Three Popular Water Models

Egor S. Kolesnikov,[†] Ivan Yu. Gushchin,[†] Petr A. Zhilyaev,[‡] and Alexey V. Onufriev[*,¶,§,‖]

[†]*Research Center for Molecular Mechanisms of Aging and Age-Related Diseases, Moscow Institute of Physics and Technology, Dolgoprudny 141700, Russia*

[‡]*Center for Design, Manufacturing and Materials, Skolkovo Institute of Science and Technology, Bolshoy Boulevard 30, bld. 1, Moscow 121205, Russia*

[¶]*Department of Computer Science, Virginia Tech, Blacksburg 24061-0131, United States*

[§]*Department of Physics, Virginia Tech, Blacksburg 24061-0131, United States*

[‖]*Center for Soft Matter and Biological Physics, Virginia Tech, Blacksburg 24061-0131, United States*

E-mail: alexey@vt.cs.edu

Overall distributions of counterions around DNA and dynamics of ions

Here we present the calculated distributions of sodium and potassium ions around double-stranded DNA for two different sequences, in simulations with four different solvent models, and two different bulk salt concentrations. These results complement those presented in the main text. Unless otherwise specified, the DNA fragment length is 25 bp, see main text.

The following detailed characteristics of the ion distributions are reported in the following tables: number of deeply bound ions (Table S1), binding affinity of ions to DNA (Table S2) and degree of DNA charge neutralisation (Table S3). The diffusion coefficients of ions are reported in Tables S4 and S5. The convergence of simulations was checked, the results are presented at Figures S6 and S5 and Table S11.

(a) polyA with NaCl

(b) mixed sequence with NaCl

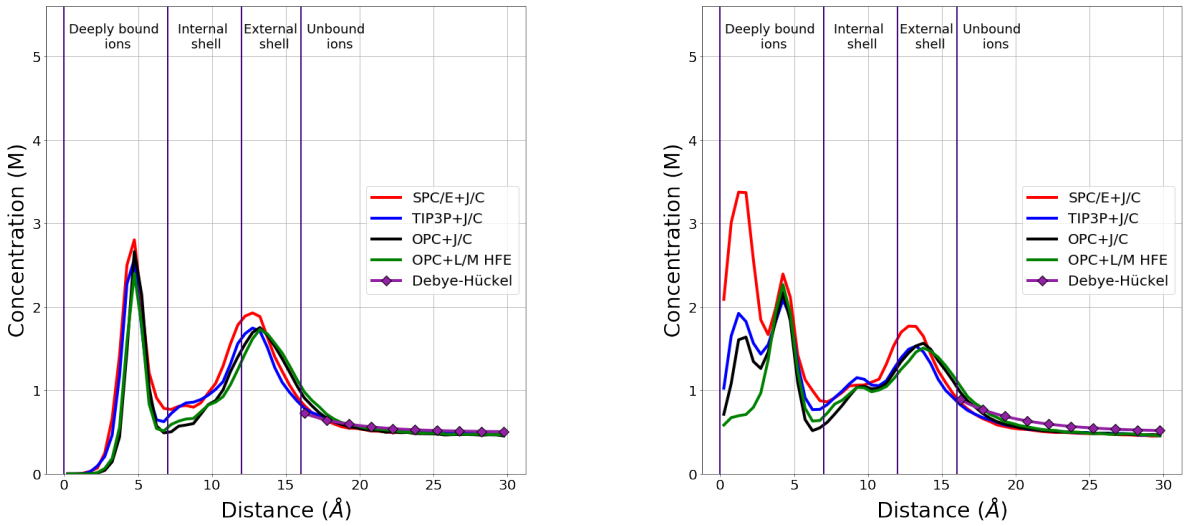

(c) polyA with KCl

(d) mixed sequence with KCl

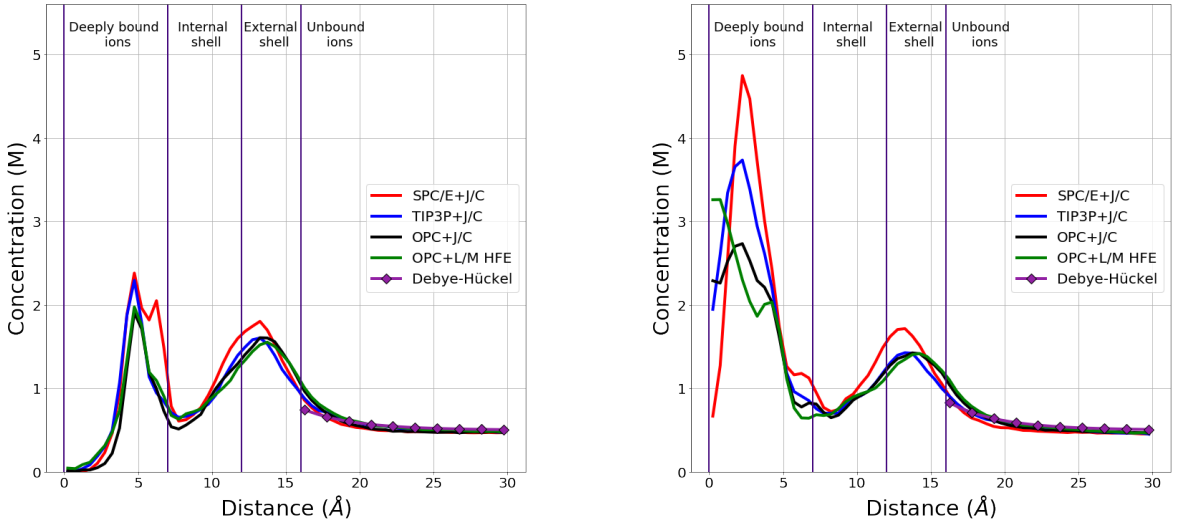

Figure S1: Dependence of sodium and potassium concentration on distance from the DNA helical axis, from simulations in four different solvent models – combinations of water models and sets of ion parameters. The bulk salt concentration is 0.5 M. All the distributions have almost the same shape beyond 7 Å from the DNA axis. In the order of solvent models SPC/E+J/C, TIP3P+J/C, OPC+J/C and OPC+L/M HFE, the ion concentration near the helical axis of DNA drops down significantly regardless of ion type and DNA sequence. The distribution corresponding to the Debye–Hückel theory is also shown for comparison. The names of the cylindrical shells around the DNA helical axis are from Ref.,[1] used here for notation convenience.

Table S1: Number of deeply bound ions in DNA simulations. In the order SPC/E+J/C, TIP3P+J/C, OPC+J/C, OPC+L/M HFE, the number of deeply bound ions decreases significantly, regardless of the ion type. The error is the standard error of the mean (see Methods).

DNA	PolyA				mixed sequence			
Bulk salt concentration (M)	0.15		0.5		0.15		0.5	
Ion type	Na^+	K^+	Na^+	K^+	Na^+	K^+	Na^+	K^+
SPC/E+J/C	5.7 ± 0.2	7.1 ± 0.1	5.8 ± 0.2	6.8 ± 0.1	6.4 ± 0.1	7.6 ± 0.1	6.7 ± 0.2	8.2 ± 0.2
TIP3P+J/C	4.1 ± 0.1	4.7 ± 0.1	4.8 ± 0.1	4.9 ± 0.1	5.1 ± 0.1	6.0 ± 0.1	5.5 ± 0.1	7.1 ± 0.1
OPC+J/C	3.3 ± 0.1	4.7 ± 0.1	4.2 ± 0.2	4.3 ± 0.1	4.4 ± 0.1	5.3 ± 0.1	4.7 ± 0.1	6.3 ± 0.1
OPC+L/M HFE	3.0 ± 0.1	4.0 ± 0.1	3.9 ± 0.2	4.6 ± 0.1	4.1 ± 0.1	4.8 ± 0.1	4.7 ± 0.1	5.7 ± 0.1

Table S2: Calculated binding affinities of Na^+ and K^+ to double-stranded DNA in different solvents. The values are in k_BT units, and the standard error of the mean is 0.02 k_BT. The binding affinity does not depend on the ion type and sequence of the DNA within the error bar.

DNA	PolyA				mixed sequence			
Bulk salt concentration (M)	0.15		0.5		0.15		0.5	
Ion type	Na^+	K^+	Na^+	K^+	Na^+	K^+	Na^+	K^+
SPC/E+J/C	−1.90	−1.92	−1.03	−1.03	−1.86	−1.88	−0.99	−1.00
TIP3P+J/C	−1.74	−1.72	−0.92	−0.87	−1.71	−1.70	−0.87	−0.84
OPC+J/C	−1.77	−1.80	−0.90	−0.89	−1.72	−1.72	−0.85	−0.84
OPC+L/M HFE	−1.75	−1.74	−0.90	−0.86	−1.73	−1.68	−0.85	−0.82

Table S3: Calculated degree of DNA charge neutralization Θ by Na^+ and K^+. Units are %, statistical error is 4%. In SPC/E+J/C, the neutralization is noticeably higher than in the other solvents. All the solvent models are qualitatively consistent with Manning's prediction,[2] but neither model matches it quantitatively at 0.15M bulk salt concentration.

DNA	PolyA				mixed sequence			
Bulk salt concentration (M)	0.15		0.5		0.15		0.5	
Ion type	Na^+	K^+	Na^+	K^+	Na^+	K^+	Na^+	K^+
SPC/E+J/C	69	72	86	86	68	68	85	84
TIP3P+J/C	59	57	77	74	58	58	74	72
OPC+J/C	62	63	79	78	58	59	75	74
OPC+L/M HFE	61	60	75	73	59	56	72	68
Manning's prediction	76	76	76	76	76	76	76	76

Table S4: Diffusion coefficients (10^{-5} cm^2/s) of sodium and potassium ions in simulations with double-stranded DNA in different solvent models. The ions move about about twice as fast in the simulations with TIP3P+J/C solvent compared to the other three solvents, where their mobility is roughly the same.

DNA	PolyA				mixed sequence			
Bulk salt concentration (M)	0.15		0.5		0.15		0.5	
Ion type	Na^+	K^+	Na^+	K^+	Na^+	K^+	Na^+	K^+
SPC/E+J/C	0.61 ± 0.01	1.02 ± 0.01	0.68 ± 0.01	1.15 ± 0.01	0.61 ± 0.01	0.99 ± 0.01	0.68 ± 0.01	1.14 ± 0.01
TIP3P+J/C	1.10 ± 0.01	1.72 ± 0.03	1.16 ± 0.01	1.87 ± 0.01	1.07 ± 0.02	1.76 ± 0.02	1.14 ± 0.01	1.86 ± 0.02
OPC+J/C	0.46 ± 0.01	0.85 ± 0.01	0.51 ± 0.01	0.94 ± 0.01	0.47 ± 0.01	0.84 ± 0.01	0.51 ± 0.01	0.94 ± 0.01
OPC+L/M HFE	0.49 ± 0.01	0.81 ± 0.01	0.53 ± 0.01	0.87 ± 0.01	0.48 ± 0.01	0.83 ± 0.01	0.54 ± 0.01	0.88 ± 0.01

Table S5: Diffusion coefficients (10^{-5} cm^2/s) of chlorine ions in simulations with double-stranded DNA in different solvent models. The ions move about about twice as fast in the simulations with TIP3P+J/C solvent compared to the other three solvents, where their mobility is roughly the same.

DNA	PolyA				mixed sequence			
Bulk salt concentration (M)	0.15		0.5		0.15		0.5	
Cation type	Na^+	K^+	Na^+	K^+	Na^+	K^+	Na^+	K^+
SPC/E+J/C	1.17 ± 0.02	1.10 ± 0.02	1.05 ± 0.01	1.10 ± 0.01	1.13 ± 0.02	1.14 ± 0.02	1.05 ± 0.01	1.10 ± 0.01
TIP3P+J/C	2.12 ± 0.05	2.06 ± 0.04	1.93 ± 0.02	1.95 ± 0.02	2.07 ± 0.04	2.03 ± 0.04	1.87 ± 0.02	1.96 ± 0.02
OPC+J/C	1.04 ± 0.02	1.07 ± 0.02	0.98 ± 0.01	1.04 ± 0.01	1.05 ± 0.02	1.04 ± 0.02	0.98 ± 0.01	1.04 ± 0.01
OPC+L/M HFE	1.12 ± 0.02	1.20 ± 0.03	1.07 ± 0.01	1.12 ± 0.01	1.16 ± 0.03	1.14 ± 0.02	1.06 ± 0.01	1.11 ± 0.01

Potassium binding sites in the DNA grooves

Tl^+ is considered a good mimic for potassium (but not for sodium) due to similar ionic radii and biophysical properties.[3] To compare simulated K^+ binding sites with the experimentally identified Tl^+ binding sites,[3] we calculated the ion density in the simulations and fitted it to the dodecamer DNA structure, see main text. We then calculated the occupancies of all the sites, and compared them with the experimentally characterized Tl^+ sites, Table S6.

Table S6: Potassium binding sites in the B-form of the Drew-Dickerson dodecamer in the MD simulations obtained using four different solvent models. Comparison of the trajectories with experimental data from Ref.[3] SPC/E water model with J/C ion parameter set shows the best agreement with experiment. 4 sym, 5 sym and 6 sym are the sites located centrally symmetrically to the 4th, 5th and 6th sites near symmetrically configured nucleotides.

Site #	area	OPC+L/M HFE	OPC+J/C	TIP3P+J/C	TIP3P+J/C, NBFIX	SPC/E+J/C	EXP
1	GC-rich, major	+	+	+	+	+	+
2							+
3	GC-rich, major	–	+	+	+	+	+
4	AT/GC-junction, minor	+	–	–	–	–	+
5	AT/GC-junction, minor	–	–	+	+	+	+
6	AT-tract, minor	–	–	–	–	–	+
7	AT-tract, minor	+	–	+	+	+	–
8	AT-tract, minor	–	–	–	–	–	+
9	GC-rich, major	+	+	+	+	+	+
10	GC-rich, major	–	+	+	+	+	+
11							+
12							+
4 sym	AT/GC-junction, minor	–	+	–	–	+	+
5 sym	AT/GC-junction, minor	–	–	–	+	+	+
6 sym	AT-tract, minor	–	–	–	–	–	+
Agreement with exp, %		27	60	53	60	67	100

Table S7: Occupancies of the ion binding sites in dodecamer structure in trajectories with 0.5 M KCl and different solvent models. Comparison with the experimental data from Ref.[3] SPC/E water model with J/C ion parameter set shows more ions in almost all of the binding sites compared to the other solvent models tested.

Site #	OPC+L/M HFE	OPC+J/C	TIP3P+J/C	TIP3P+J/C, NBFIX	SPC/E+J/C	EXP	Site # in exp
1	0.15 ± 0.02	0.18 ± 0.03	0.24 ± 0.03	0.22 ± 0.03	0.26 ± 0.04	0.1	8
2						0.1	7
3	0.09 ± 0.02	0.11 ± 0.02	0.17 ± 0.02	0.23 ± 0.04	0.19 ± 0.03	0.2	3
4	0.13 ± 0.04	0.01 ± 0.01	0.04 ± 0.02	0	0.06 ± 0.02	0.12	9
5	0.05 ± 0.02	0	0.19 ± 0.04	0.24 ± 0.04	0.32 ± 0.04	0.18	5
6	0	0	0	0	0	0.2	4
7	0.13 ± 0.04	0	0.10 ± 0.03	0.27 ± 0.05	0.21 ± 0.05	0	–
8	0	0	0	0	0	0.1	6
9	0.12 ± 0.01	0.13 ± 0.03	0.18 ± 0.01	0.25 ± 0.03	0.18 ± 0.02	0.34	1
10	0.09 ± 0.02	0.20 ± 0.03	0.28 ± 0.03	0.27 ± 0.03	0.30 ± 0.04	0.15	10
11						0.16	13
12						0.29	2
4 sym	0.025 ± 0.007		0.08 ± 0.03	0.23 ± 0.04	0.70 ± 0.04	0.12	–
5 sym	0.016 ± 0.004	0.05 ± 0.02	0.06 ± 0.02	0	0.44 ± 0.04	0.18	–
6 sym	0	0	0	0	0	0.2	–

Experiment shows that Tl^+ ions tend to occupy binding sites in the minor groove of AT-tract and the major groove of GC-rich areas of DNA.[3] To compare results obtained using our simulations of 25 bp long DNAs with this experimentally characterized trend, we calculated the numbers of potassium ions in minor groove of AT-tract and the major groove of GC-rich areas of simulated DNA duplexes, Tables S8 and S9. Mindful of the caveats on quantitative interpretation of these experiments, see main text, we can conclude that OPC + L/M HFE likely underestimates K^+ binding occupancy in the minor grove of the AT-tract – at both bulk salt concentrations, including 0.5M, the corresponding calculated occupancy is negligible. All the four solvent models show almost the same number of potassium ions in the major grooves of GC-rich regions of simulated mixed sequence DNA (see Table S9).

Table S8: Numbers of potassium ions in minor grooves of polyA DNA, and in the AT-tract of the mixed sequence DNA. SPC/E water with J/C ion parameter set shows more ions than other water/ion combinations, virtually independent of the ion type, and bulk salt concentration.

DNA	PolyA		mixed sequence, TATAAAA	
Bulk salt concentration (M)	0.15	0.5	0.15	0.5
SPC/E+J/C	2.6 ± 0.1	1.7 ± 0.1	0.21 ± 0.05	0.35 ± 0.04
TIP3P+J/C	0.60 ± 0.06	0.41 ± 0.05	0.20 ± 0.03	0.19 ± 0.03
OPC+J/C	1.25 ± 0.06	0.44 ± 0.07	0.05 ± 0.02	0.21 ± 0.05
OPC+L/M HFE	0.74 ± 0.02	0.55 ± 0.08	0.06 ± 0.02	0.04 ± 0.01

Table S9: Numbers of potassium ions in major grooves of different GC-rich parts of the mixed sequence DNA. SPC/E water with J/C ion parameter set shows slightly more ions than other combinations, virtually independent of the ion type and bulk salt concentration.

	mixed sequence, GGGC		mixed sequence, GGGCG	
Bulk salt concentration (M)	0.15	0.5	0.15	0.5
SPC/E+J/C	0.36 ± 0.02	0.65 ± 0.03	0.95 ± 0.04	0.90 ± 0.03
TIP3P+J/C	0.51 ± 0.02	0.45 ± 0.02	0.84 ± 0.03	0.80 ± 0.02
OPC+J/C	0.24 ± 0.01	0.38 ± 0.02	0.81 ± 0.03	0.77 ± 0.04
OPC+L/M HFE	0.18 ± 0.02	0.53 ± 0.03	0.73 ± 0.04	0.78 ± 0.03

Na^+ vs. K^+ binding to DNA

We also compared the behavior of sodium and potassium ions around the Drew–Dickerson dodecamer (CGCGAATTGCGC). In particular, we were interested to determine whether Na^+ has any binding sites coinciding with the K^+ sites. To answer this question, we simulated a trajectory of the dodecamer in 0.5M NaCl in SPC/E water with the J/C ion set for 100 ns (see details in Methods). The differences between the ion distributions are seen in the radial-angle distributions of potassium vs. sodium molarities (Figure S2).

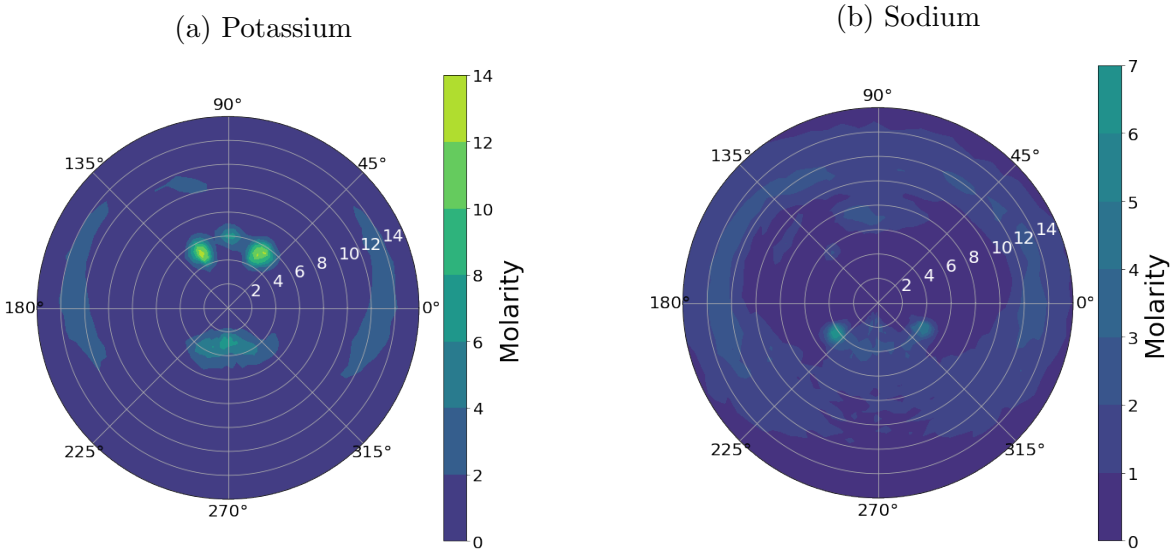

Figure S2: Radial-angle distributions of sodium and potassium concentrations around DNA dodecamer in SPC/E water model with J/C ion parameter set. In constrast to K^+, localization of Na^+ to specific sites is much less pronounced. Numbers inside the circles show distance from the helical axis. Same colors correspond to the same molarity.

Near the potassium binding sites, the concentration of potassium reaches much larger values than in the case of sodium binding. The most occupied sodium binding site is found in the major groove of AT-tract and its occupancy is 0.12 ± 0.03 (see Figure S2b). At the same time, in the system with potassium, there are 8 distinct binding sites (see Figure S2a and Tables S6 and S7).

These results show that details of local distribution near the electronegative binding sites depend on the type of ion significantly in SPC/E+J/C solvent. Earlier it was found

that sodium is much less concentrated in major groove of DNA than potassium,[4] where the most occuped monovalent binding sites were experimentally found (see Table S7). In our simulations sodium is also less concentrated in major groove of DNA than potassium (see Figure S2).

Dependence of ion distributions on the DNA force field

To investigate possible dependence of the ion distributions on the force field used, we simulated the 25 bp mixed sequence DNA in OPC+L/M HFE solvent model and 0.15 M salt in force field ff99bsc1,[5] to compare with the main text results based on ff99bsc0.

(a) NaCl (b) KCl

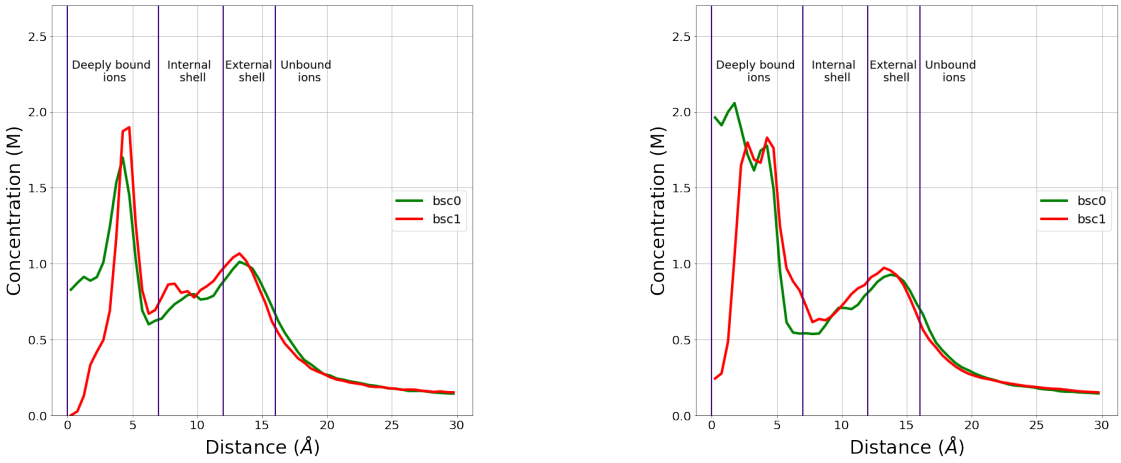

Figure S3: Dependence of radial distributions of ions on DNA force field. Here we used mixed sequence in OPC+L/M HFE solvent model, bulk salt concentration is 0.15 M. Distribution of ions close to the helical axis of DNA depends on the employed DNA force field. The names of the cylindrical shells around the DNA helical axis are from Ref.,[1] used here for notation convenience.

As can be seen from Figure S3, the ion distributions very near the helical axis are highly sensitive to the choice of force-field. In interpreting potential significance of this result one should be mindful of the following. The ion concentration near the helical axis is determined by the ratio between number of ions no further than 1-2 Å and the curved tube's volume with the axis coinciding with the helical axis of DNA and with radii 1-2 Å. A small change of the number of ions near the axis can cause considerable change in the corresponding ion concentration.

To further quantify the sensitivity to the force-field, we have computed the cumulative function of potassium ion distribution, see Table S10. These results show that the total number of deeply bound ions does not depend on the DNA force field significantly.

Stronger claims will require a much more thorough additional investigation, which is beyond the scope of this work focused on solvent models.

Table S10: Cumulative number of potassium ions in cylindrical shells of increasing radii around the helical axis. Dependence on the force-field: ff99bsc0 vs. ff99bsc1. System with mixed sequence sequence in 0.15 M solution of KCl in OPC water model with L/M HFE ion parameter set was used to check the dependence on the force field. The total number of deeply bound ions (indicated in bold) is not very sensitive to the DNA force field, but their distribution very near the DNA axis is.

Shell radius, Å	ff99bsc0	ff99bsc1
1	0.13 ± 0.02	0.02 ± 0.01
2	0.56 ± 0.04	0.16 ± 0.02
3	1.23 ± 0.06	0.70 ± 0.04
4	2.16 ± 0.09	1.54 ± 0.06
5	3.3 ± 0.1	2.77 ± 0.08
6	4.06 ± 0.1	3.94 ± 0.1
7	**4.80±0.14**	**5.1±0.1**
8	5.66 ± 0.14	6.21 ± 0.14
9	6.72 ± 0.14	7.35 ± 0.1

All-atom MD simulations

Figure S4 shows a typical simulated system.

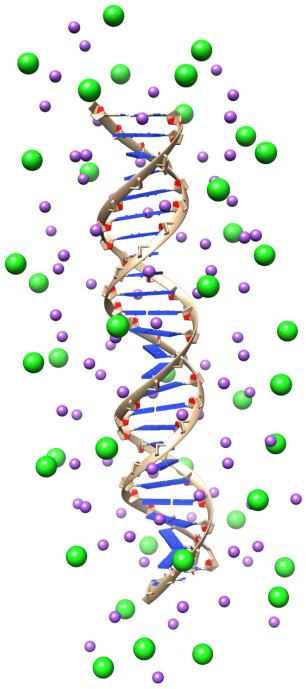

Figure S4: The DNA-ion system at the start of a simulation. Magenta spheres are sodium ions, green spheres are chlorine ions. Bulk salt concentration is 0.15 M. Water molecules are hidden for clarity.

Convergence of ion distributions

We varied the volume of the simulation box 4-fold, and the simulation time 10-fold, to check if the computed distributions of ions change. For this test, we chose the systems with mixed sequence DNA, TIP3P water model, J/C ion parameters set. For the 0.15M salt simulation, we quadrupled the solvent box volume by doubling the dimensions of the box in the directions perpendicular to the helical axis of the DNA. For the system in the standard box, with 0.5 M bulk salt concentration, where more ions are expected to bind, we extended the simulation time to 1 microsecond, and compared the distributions obtained from the first 100 ns of

the trajectory with those averaged over the whole trajectory. Comparison of the calculated distributions averaged over different time windows, and with different sizes of the solvent box, are presented below.

Table S11: Dependence of the number of deeply bound ions on the simulation parameters. Mixed sequence, 25 bp long DNA. Solvent model is TIP3P+J/C. None of the changes in the simulation parameters cause noticeable changes in the number of deeply bound ions.

Bulk salt concentration (M)	0.15		0.5	
Ion type	Volume of box		Averaging time window for standard box	
	Standard	Quadrupled	0-100ns	0-1000ns
Na^+	5.1 ± 0.1	5.0 ± 0.1	5.5 ± 0.1	5.7 ± 0.1
K^+	6.0 ± 0.1	6.3 ± 0.1	7.1 ± 0.1	7.0 ± 0.1

(a) NaCl

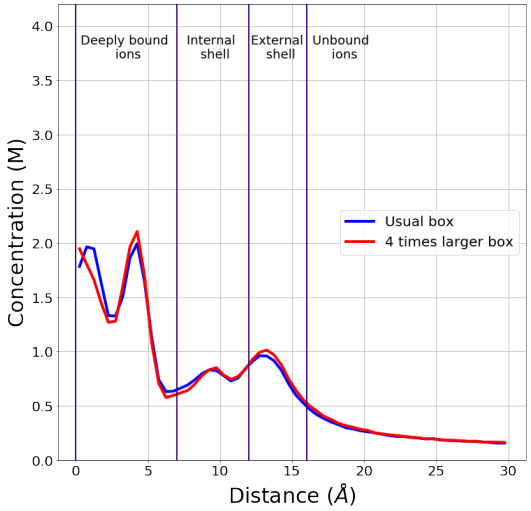

(b) KCl

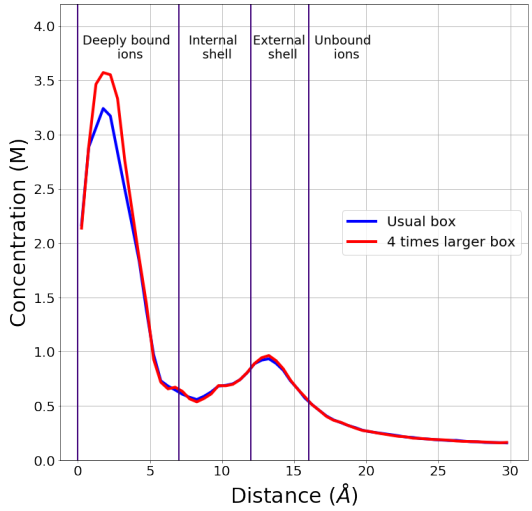

Figure S5: Radial distributions of monovalent ions around dsDNA are virtually independent of the simulation box size. Shown are results for mixed sequence in TIP3P water model with J/C ions, 0.15 M bulk salt concentration. The cylindrical shells around the DNA are as in Figure 1 at the main text.

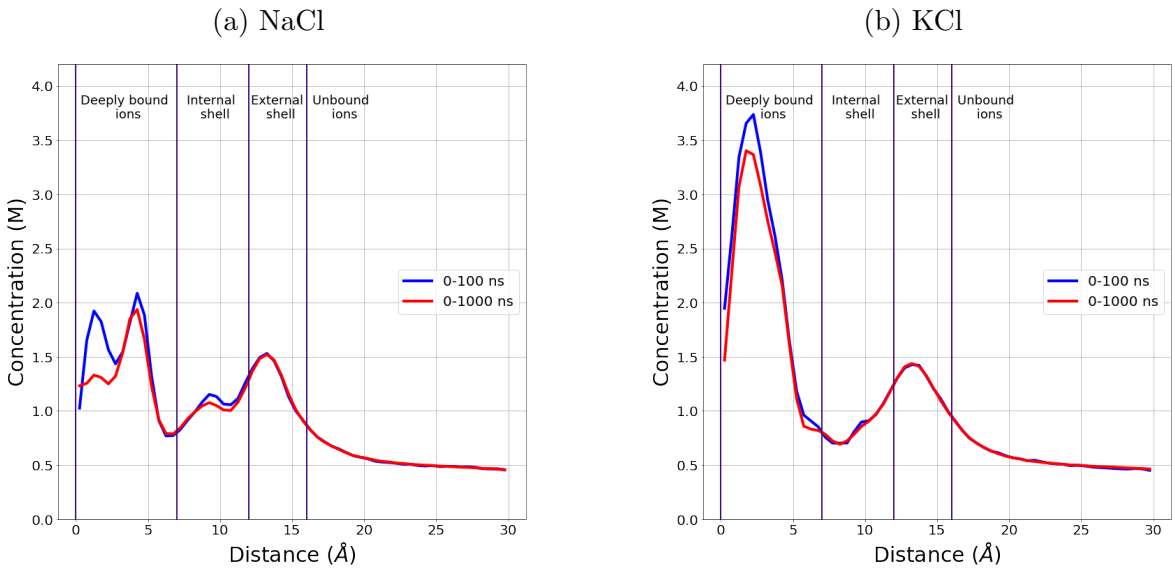

Figure S6: Dependence of radial distributions of ions on the averaging time (production trajectory length): 100 ns (blue) vs. 1000 ns (red). The distributions show weak dependence on the averaging time, confirming acceptable convergence at 100ns. Mixed sequence, 25 bp long DNA fragment in TIP3P water model with J/C ions, 0.5 M bulk salt concentration. The cylindrical shells around the DNA are as in Figure 1 in main text.

Estimation of values and their statistical errors

To estimate statistical (sampling) errors, we use the slicing method.[6] First, we count the number of deeply bound ions in every snapshot along the trajectory. Then, we plot the distribution of the number of snapshots containing the given number of deeply bound ions. We find where the distribution reaches half of its maximum value; we take those two numbers of deeply bound ions as the thresholds, Figure S7. Then we count the number of pieces of the trajectory, in each of which the number of deeply bound ions crosses each of the threshold values at least ones (in our case their number was 63, we round it to $N = 50$). After that we cut the trajectory onto $N = 50$ equal 2 ns-long fragments, and calculate the corresponding average number of deeply bound ions, binding affinity of ions to DNA and other reported values. The standard deviation σ is computed, and the assigned error is the standard error of the mean $\sigma/\sqrt{N}$.

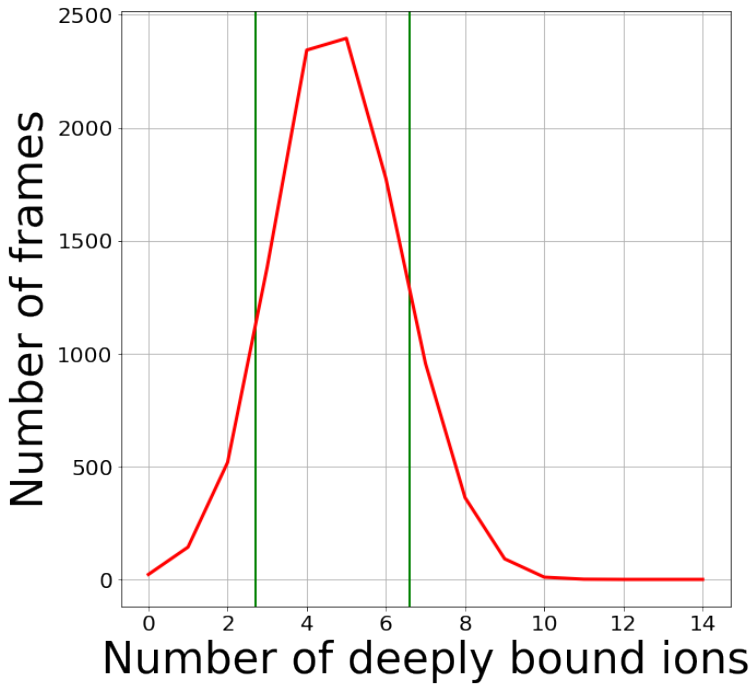

Figure S7: Distribution of the number of snapshots containing the given number of deeply bound ions. Trajectory of mixed sequence in OPC+L/M HFE and 0.15M KCl, length is 100 ns. Vertical green lines intersect the distribution curve at half its maximum value.

Occupancy of ion binding sites in simulations

To estimate the occupancy of each binding site, we first define its dimensions as half width of the ion density distribution around the site, Figure S8. Specifically, we generate the ion density distribution as a function of three coordinates: distance from the DNA helical axis, angle, and the distance along the DNA axis (exemplified in Figure S8 for K^+ binding site # 1 in SPC/E water). Along each coordinate, the boundaries of the binding site are defined as the points where the ion density equals half of its maximum value. Once the boundaries are defined, we count the number of ions observed within the binding site along the simulated trajectory.

Calculation of the degree of DNA neutralization

To calculate the degree of DNA charge neutralization we used the following equation:

(a) Dependence on coordinate along DNA axis

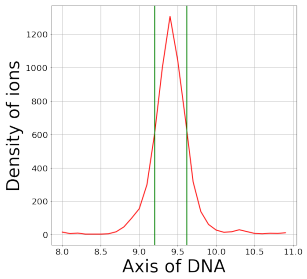

(b) Dependence on angle

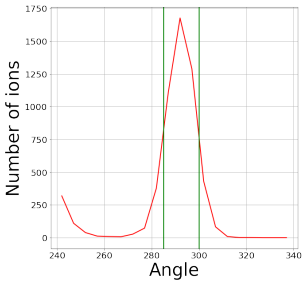

(c) Dependence on distance from DNA axis

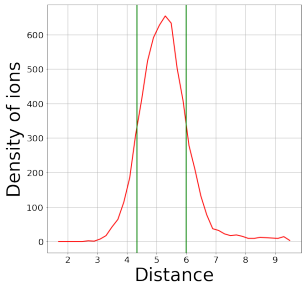

Figure S8: Ion density distribution around the binding site 1 in simulations of the Drew-Dickerson dodecamer in SPC/E+J/C as a function of distance from the DNA helical axis (a), angle (b), and the distance along the DNA axis (c). Vertical lines correspond to coordinates where the function reaches half of its maximum value. Binding site is defined as located between those coordinates.

$$D = \frac{|Q_{DNA}| + N_- - N_+}{|Q_{DNA}|} \cdot 100, \tag{1}$$

where D is a degree of DNA charge neutralization, $|Q_{DNA}| = 48$ is DNA charge, N_- is number of Cl^- ions that are closer than 16 Å to DNA helical axis, N_+ is a number of positively charged ions (Na^+ or K^+) that are closer than 16 Å to DNA helical axis.

To avoid edge effects we have decided not to consider several nucleotides at both ends of the DNA in the calculation of the degree charge neutralization. To estimate reasonable number of nucleotides needed to be excluded, we calculate the degree of charge neutralization (Θ or Theta) with different numbers of excluded nucleotides in one of our systems (polyA in SPC/E+J/C, 0.15M NaCl).

As we can see, the degree of charge neutralization does not change dramatically after exclusion of two nucleotides at the ends of the DNA duplex. Thus, we have excludes two nucleotides in our calculations of the degree of charge neutralization.

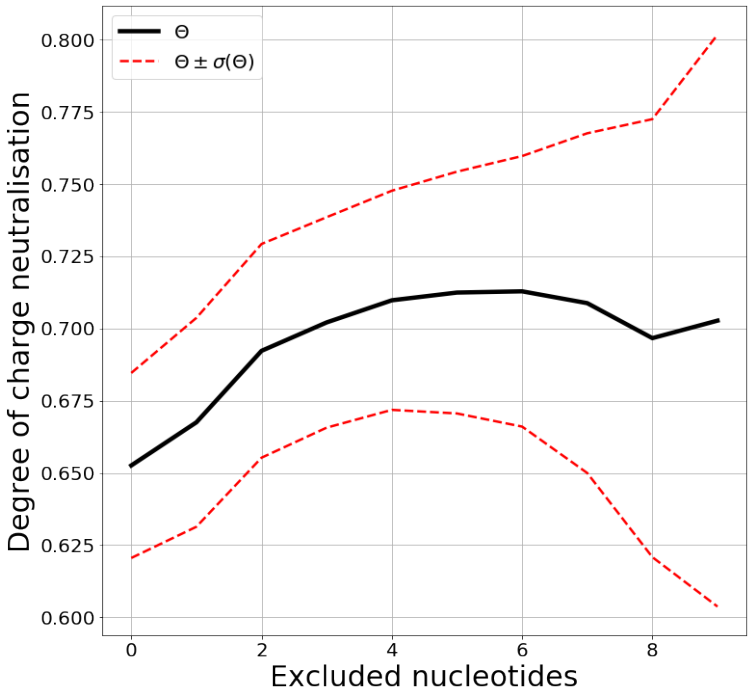

Figure S9: Dependence of the degree of neutralization of the DNA by counter-ions, Θ, on the number of nucleotides excluded from the calculation of Θ. Here, $\sigma(\Theta)$ is the statistical error of Θ. The degree of neutralization Θ does not increase significantly beyond 2 excluded nucleotides, but its statistical error does.

References

(1) Tolokh, I.; Pabit, S.; Katz, A.; Chen, A.; Drozdetski, A.; Baker, N.; Pollack, L.; Onufriev, A. Why double-stranded RNA resists condensation. *Nucleic acids research* **2014**, *42*.

(2) Manning, G. S. Limiting Laws and Counterion Condensation in Polyelectrolyte Solutions II. Self-Diffusion of the Small Ions. *The Journal of Chemical Physics* **1969**, *51*, 934–938.

(3) Howerton, S. B.; Sines, C. C.; VanDerveer, D.; Williams, L. D. Locating Monovalent Cations in the Grooves of B-DNA,. *Biochemistry* **2001**, *40*, 10023–10031.

(4) Yoo, J.; Aksimentiev, A. Competitive Binding of Cations to Duplex DNA Revealed through Molecular Dynamics Simulations. *The Journal of Physical Chemistry B* **2012**, *116*, 12946–12954.

(5) Ivani, I. et al. Parmbsc1: a refined force field for DNA simulations. *Nature methods* **2016**, *13*, 55–58.

(6) Straatsma, T.; Berendsen, H.; Stam, A. Estimation of statistical errors in molecular simulation calculations. *Molecular Physics* **1986**, *57*, 89–95.